Available online at www.sciencedirect.com

SciVerse ScienceDirect

Ceramics International 39 (2013) 6735–6741

CERAMICS INTERNATIONAL

www.elsevier.com/locate/ceramint

Study of cation distribution for Cu–Co nanoferrites synthesized by the sol–gel method

Imran Ahmad[a,*], Tahir Abbas[a], M.U. Islam[a], Asghari Maqsood[b]

[a]Department of Physics, Bahauddin Zakariya University, Multan 60800, Pakistan
[b]Centre for Emerging Sciences, Engineering and Technology (CESET), I 10/3 Islamabad 45320, Pakistan

Received 22 October 2012; received in revised form 19 January 2013; accepted 1 February 2013
Available online 10 February 2013

Abstract

Nano sized polycrystalline soft ferrite particles with composition $Cu_{1-x}Co_xFe_2O_4$ (x =0.1, 0.3, 0.5, 0.7, 0.9) were synthesized by the sol–gel technique. The existence of well-defined single cubic spinel structure was confirmed in all the samples by X-ray diffraction. The crystallite size found by XRD varied from 14.8 to 34.0 nm. The microstructure was also characterized by scanning electron microscopy (SEM) and transmission electron microscopy (TEM). Slight expansion of the unit cell was detected with the increase of Cobalt concentration, which may be attributed due to larger ionic radius of Co^{2+}. Lattice parameter ranged from 8.34 Å to 8.37 Å for Co^{2+} from 0.1–0.9. The distribution of cations amongst A- and B-sites of the lattice was estimated by X-ray diffraction by using the R-factor technique. The results showed that both Cu^{2+} and Co^{2+} ions occupy mainly the B-site while Fe^{3+} ions were equally distributed among A- and B-sites. The data obtained from cation distribution analysis was used to determine the magnetic moment for each sample and VSM studies were also carried out to validate these calculations. Magnetic measurements showed that the saturation magnetization (Ms) and coercivity (Hc) increased with increasing cobalt content.

Keywords: D. Ferrites; Cation distribution; Sol–gel; X-ray diffraction

1. Introduction

Spinel ferrites have numerous applications in different fields due to their significant structural, electrical and magnetic properties. Estimation of the cation distribution is of huge importance because the hypothetical explanation of the chemical and physical properties of these oxides depends upon the distribution of cations amongst A- and B-sites of the lattice [1]. Site preference of cations is strongly related to the factors like ionic radius, crystal and ligand fields, electronic configuration and anion polarization [2]. Cubic spinel ferrites (space group Fd3m) have either of the two structures: the normal spinel or the inverse spinel.

The spinels having all the divalent cations (Me^{2+}) on the A-sites and trivalent cations (Me^{3+}) on the B-sites are called the normal spinels i.e.$Me^{2+}[Me^{3+}]$ O_4 and those with divalent cations (Me^{2+}) on the B-sites and equally distributed trivalent cations (Me^{3+}) among the A- and B-sites are called the inverse spinels i.e. $Me^{3+}[Me^{2+}$ $Me^{3+}]$ O_4 [3].

Many techniques have been used for the determination of cation distribution by using the X-ray diffraction such as R-factor [4,5], Furuhashi [6] and Bertaut methods [7]. The additional techniques include neutron diffraction [8], thermoelectric measurements [9], and electron spin resonance [10]. The intensity of X-ray reflections reveals a reliance on the possession of cations amongst the interstitial sites. So all of the above said methods in which X-ray diffraction has been used, are based upon the comparison of experimentally observed intensities with those, calculated for the hypothetical crystal structure [11]. Cobalt ferrite is reported as an inverse spinel and the degree of inversion is strongly dependent on the preparation conditions and methods [12,13]. The distribution of cations in copper ferrites, prepared by co-precipitation technique is reported as

*Corresponding author. Tel.: +92 30 16790448.
E-mail address: imraan77@yahoo.com (I. Ahmad).

0272-8842/$ - see front matter © 2013 Elsevier Ltd and Techna Group S.r.l. All rights reserved.
http://dx.doi.org/10.1016/j.ceramint.2013.02.001

$Cu_{0.2}$ $Fe_{0.8}$ [$Cu_{0.8}$ $Fe_{1.2}$] O_4. Although a lot of work has been done on $CoFe_2O_4$ and $CuFe_2O_4$, a little work is found in literature on mixed Co–Cu ferrites. Tailhades et al. [14] prepared mixed cobalt–copper spinel ferrites $Co_xCu_{1-x}Fe_2O_4$ with acicular shape from oxalate precursors and reported that the cation distribution is sensitive to the thermal history of the samples. However, there is no reported work in the literature for the cation distribution of mixed Co–Cu ferrites prepared through the sol–gel route. The aim of this work was to prepare Co–Cu ferrites by the sol–gel method and to estimate cation distribution in these ferrites. In the present work, the R-factor method has been used to calculate the distribution of cations.

2. Experimental

Polycrystalline ferrites of the formula $Co_xCu_{1-x}Fe_2O_4$ (where $x=0.1$, 0.3, 0.5, 0.7, 0.9) were prepared by the sol–gel (auto-combustion) method. Stoichiometric amounts of metal nitrates and citric acid were first dissolved into deionized water to form a mixed solution. The molar ratio was fixed as 1:1 of nitrates to citric acid. The homogenous distribution and segregation of the metal ions was achieved by the use of citric acid. In order to speed up the reaction the pH value of the solution was maintained between the range of 7–8 by drop wise addition of ammonia solution (base catalyst) [15]. The solution was constantly stirred using a magnetic agitator and formation of a polymer complex took place through condensation reaction between the metal nitrates and the molecules of citrates [16]. Then the obtained sol was heated at 135 °C on hot plate under regular stirring to condensate it into a dried gel. Additional heating led to the ignition of the dry gel and a loose ferrite nanopowder was obtained through the burning of the gel in a self-propagating combustion manner. During the combustion process, exothermic decomposition of a redox mixture of the metal nitrates and citric acid took place along with the removal of a large amount of gases such as N_2, H_2O, and CO_2. The prepared powder samples were then annealed for 5 h at 500 °C in order to enhance the crystallinity. The processing steps involved are shown in Fig. 1. The X-ray diffraction was used to characterize the samples for their structure, density and average particle size. X-ray diffractometer (PANalytical) with Cu-Kα radiation (wavelength $\lambda=1.5406$ Å) was used for this purpose.

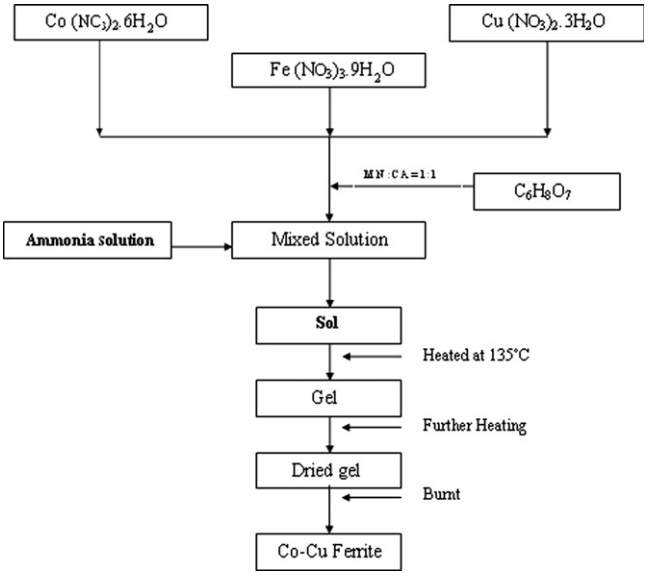

Fig. 1. Schematic of the preparation of Co–Cu nanoferrites.

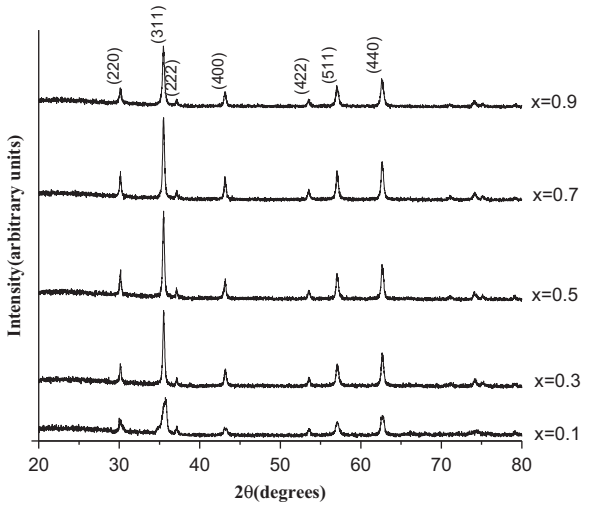

Fig. 2. X-ray diffraction pattern of $Co_xCu_{1-x}Fe_2O_4$ ferrite system.

3. Results and discussion

3.1. Structural studies

The XRD patterns of the $Co_xCu_{1-x}Fe_2O_4$ ferrite system (with $X=0.1$, 0.3, 0.5, 0.7, 0.9) are shown in Fig. 2. Indexing was carried out for the confirmation of fcc cubic spinel structure. It was found that all the compositions have a well-defined crystalline fcc cubic phase and there is no indication of the development of mixed phases. Substitution of Cu with Co increased the overall crystallinity of the spinel phase [17]. The observed XRD peaks, interplaner spacing and corresponding crystal planes of each composition were recorded. Linear increase in the lattice constant by the increase of Co^{2+} ion concentration in Co–Cu ferrites was observed, which follow the Vegard's law [18] and is shown in Fig. 3. This increase is due to the difference in cationic radii of Co^{2+} (0.82 Å) and Cu^{2+} (0.70 Å) ions. Substitution of larger Co^{2+} ions with relatively smaller Cu^{2+} ions causes the slight expansion of unit cell. Lattice constant values, calculated using the standard equation, are given in Table 1.

$$a = d(h^2+k^2+l^2)^{1/2}$$

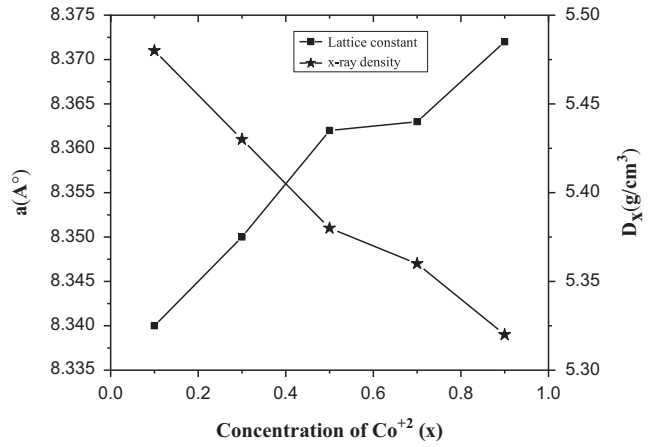

Fig. 3. Variation of Lattice parameter and X-ray density as a function of Co content.

Table 1
Lattice constant, particle size, X-ray density of $Co_xCu_{1-x}Fe_2O_4$.

Composition (x)	0.10	0.30	0.50	0.70	0.90
Lattice constant (Å)	8.340	8.350	8.362	8.363	8.372
Particle size (nm)	14.80	33.60	34.00	33.20	29.20
X-ray density (g/cm^3)	5.48	5.43	5.38	5.36	5.32

Reported lattice constant value of copper ferrites (co-precipitation method) is 8.371 Å [19] and of cobalt ferrites (sol–gel method) is 8.377 Å [20]. In the case of our samples while moving towards the copper ferrite side the lattice parameter values were found to be slightly lesser than the reported ones. The reduced lattice parameters might be occurred due to the sol–gel method. X-Ray density values for all the compositions were calculated from the following relation (Table 1).

$$D_x = 8M/Na^3$$

M is the molecular weight, N is Avogadro's number ($=6.0225\times10^{23}$ atom/mole) and 'a' is the lattice constant. '8' stands for the number of formula units/cell. The decreasing trend in X-ray density is due to the increase in volume and gradual decrease in mass as well (Fig. 3).

By the use of classical Scherrer formula [21], average size of the prepared ferrite particles was determined:

$$D_{hkl} = 0.9\lambda/B\cos\theta$$

where, D_{hkl} is the particle size found from (3 1 1) peak, B is full width of the peak at half- maximum intensity (radians), and λ is the wavelength of x-ray (1.5406 Å).

SEM and TEM micrographs (Figs. 4–5) show that the samples of $Cu_{1-x}Co_xFe_2O_4$ ($x=0.1$, 0.5 and 0.9) are composed of nanoparticles with dimensions ranging from 20 to 55 nm. The larger size of the nanoparticles compared to the values given by the Scherrer formula may be caused by the agglomeration.

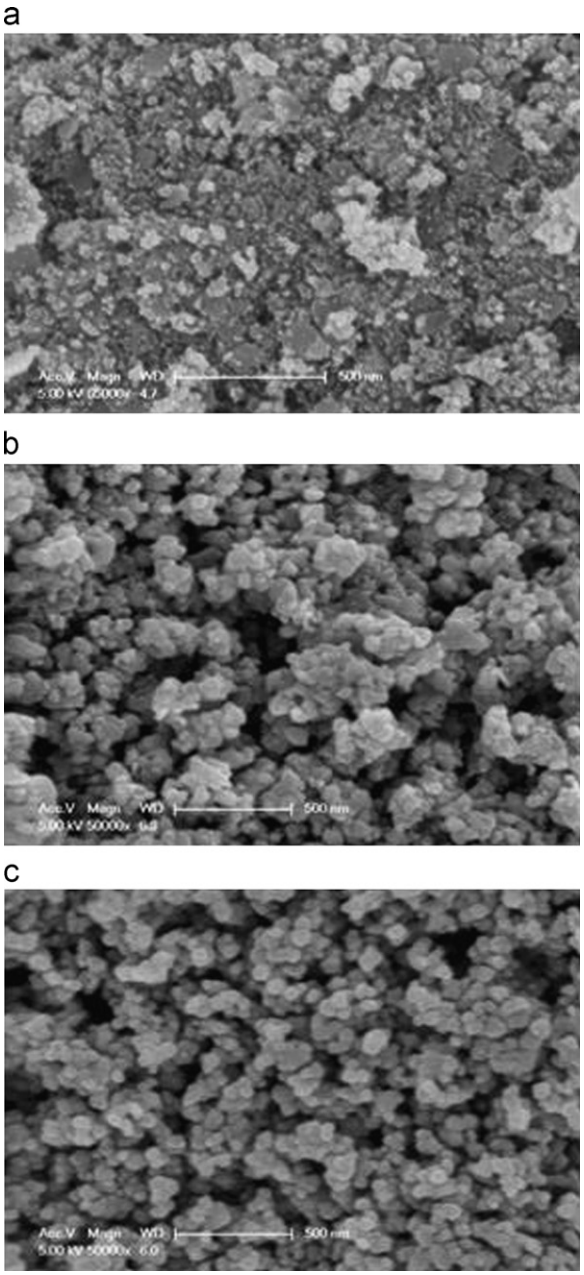

Fig. 4. (a–c) Scanning electron micrographs of $Cu_{1-x}Co_xFe_2O_4$ (for $x=0.1$, 0.5 and 0.9) ferrite nanoparticles.

3.2. Estimation of the site occupancy of cations

The X-ray diffraction, in combination with the computational technique can be used to calculate the degree of inversion and oxygen positional parameter [5]. A computer program based upon the R-factor method was formulated to determine the distribution of cations over tetrahedral-A and octahedral-B-sites in the fcc lattice of a Co–Cu ferrite system. R-factor method works for the selection of best structure by diminishing the value of residual function, R, and it provides

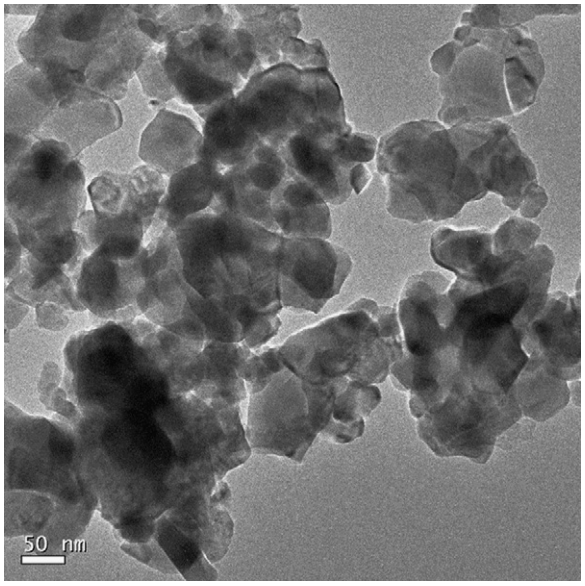

Fig. 5. TEM micrograph of $Co_{0.5}Cu_{0.5}Fe_2O_4$ nanoparticles.

the simultaneous calculation of cation distribution, oxygen positional parameter and thermal scale factor. The minimum value of residual function R was required, so the program was run for 10–100 iterations until the least value was reached.

Expressions for the residual function R are as under:

$$R_1 = \frac{\sum_{hkl}\left|I_{hkl}^{obs} - I_{hkl}^{cal}\right|}{\sum_{hkl} I_{hkl}^{obs}}$$

$$R_2 = \frac{\sum_{hkl}\left|\sqrt{I_{hkl}^{obs}} - \sqrt{I_{hkl}^{cal}}\right|}{\sum_{hkl}\sqrt{I_{hkl}^{obs}}}$$

where I_{hkl}^{obs} *and* I_{hkl}^{cal} are the observed and calculated intensities for *hkl* reflections. For the calculation of the relative integrated intensity of a specified diffraction line, the following formula is pertinent.

$$I_{hkl} = |F|^2 P L_P$$

where F is the structure factor, P, the multiplicity factor and L_p is the Lorenz-polarization factor. For the structure factor calculations, the atomic scattering powers for various ions were taken from the literature. In our intensity calculations temperature correction was not necessary because in spinels, the thermal vibration of the atoms at room temperature should not differ greatly from that at absolute zero [11].

The spinel structure consists of a cubic closed-pack arrangement of 32 oxygen ions, forming an fcc lattice with two types of interstitial sites. Eight out of 64 tetrahedral sites (A-sites) and 16 out of 32 octahedral sites (B-sites) are occupied by the cations [22]. Each A-site is surrounded by 4 oxygen ions and B-site by 6 oxygen ions. To calculate the structure factors, complete understanding of the geometry of spinel structure is required. The most of the compounds having spinel structure fit in to the space group Fd3m (O_h^7, number 227 in the International Tables) with the cations occupying the special positions 8a and 16d and anions the universal positions 32e [22].The origin is taken on $\bar{4}3$ m at A-site cation and positional coordinates of the filled lattice sites of the cubic unit cell are given in the Table 2. The general formula used to find the distribution of cations amongst the tetrahedral A-sites and octahedral B-sites can be expressed as [23].

$$Me_{\delta}^{2+}Fe_{1-\delta}^{3+}\,[Me_{1-\delta}^{2+}\,Fe_{1+\delta}^{3+}]\,O_4$$

where the square brackets are used for the octahedral cations, and the tetrahedral ones are given infront of the square brackets, δ is a measure of the inversion (distribution) parameter and depends upon the conditions for the preparation. $\delta=0$, for an inverse spinel, $\delta=1$, for a normal spinel, $0<\ \delta<1$ for intermediate spinels and Me is representing here a divalent cation or a combination of divalent cations. The values of inversion parameters δ, oxygen positional parameters u and the residual functions R, for all the prepared compositions of Co–Cu ferrite system are tabulated in the Table 3.

The ideal u parameter values for a perfect cubic closed-pack arrangement of anions are 3/8(0.375) and 1/4(0.250), for origins at $\bar{4}3$ m and $\bar{3}$ m (center of symmetry), respectively [22]. By the variation of the value of u, expansion or contraction of the anion sub lattice takes place awaiting the volume of A- and B-site match the radii of the constituent cations. The value of u is greater than 0.375 for this case.

Estimated cation distribution for these samples, shown in the Table 3, clearly indicates that both Cu and Co ions are distributed over the B-sites and Fe ions are evenly dispersed among A- and B-sites.

3.3. The interionic distances

Cation-anion distances at the A-site (tetrahedral bond) and the B-site (octahedral bond) are calculated by inserting the values of lattice parameter 'a' and positional oxygen parameter 'u' in the following eqns. [21]:

$$d_{TL} = a\sqrt{3}(\mathrm{u}-0.25) \qquad (\mathrm{tet-bond})$$
$$d_{OL} = a(3\mathrm{u}^2 - 11/4\mathrm{u} + 43/64)^{1/2} \quad (\mathrm{oct-bond})$$

Anion–anion distances can be calculated using the next eqns.

$$d_{TE} = a\sqrt{2}(2\mathrm{u}-1/2) \qquad (\mathrm{tet-edge})$$
$$d_{OE} = a\sqrt{2}(1-2\mathrm{u}) \qquad (\mathrm{sharedoct-edge})$$
$$d_{OEU} = a(4\mathrm{u}^2 - 3\mathrm{u} + 11/16)^{1/2} (\mathrm{unsharedoct-edge})$$

Cation–cation distances at A- and B-sites are calculated using the following eqns.

$$d_A = a\sqrt{3}/4$$
$$d_B = a\sqrt{2}/4$$

Obtained values are listed in the Table 4.

3.4. Magnetic moments

The net magnetic moments of the spinel can be calculated on the basis of occupancy of cations among A- and B-sites of the lattice. The magnetic moments of both the A-site and B-site cations counter each other in an applied magnetic field. The ionic magnetic moments of Fe^{3+}, Cu^{2+} and Co^{2+} are 5 μ_B, 1 μ_B and 3 μ_B respectively. The net magnetic moment values collected on the basis of cation distribution (A–B interactions) are listed in the Table 5 and are in good consistency with the values calculated from magnetic measurements..

3.5. Magnetic studies

Magnetization measurements at room temperature were carried out for $Cu_{1-x}Co_xFe_2O_4$ ($x=0.1$ and 0.9) using VSM with the maximum applied field of 25 kOe. The

Table 2
Positional coordinates of the filled lattice sites.

Lattice site	Equipoint	Point symmetry	Fractional coordinates of lattice sites
			Origin on $\bar{4}$3 m at A-site cation (1/8,1/8,1/8 from $\bar{3}$m on octahedral vacancy) (0, 0, 0; 0,1/2,1/2; 1/2,0,1/2; 1/2,1/2, 0)+
A-site cation	8a	$\bar{4}$3 m	0, 0, 0; ¼,1/4,1/4
B-site cation	16d	$\bar{3}$m	5/8,5/8,5/8; 5/8,7/8,7/8; 7/8,5/8,7/8; 7/8,7/8,5/8
Anions	32e	3 m	*u*, *u*, *u*;u,$\bar{u}$,$\bar{u}$; (1/4 –u),(1/4-u),(1/4-u);(1/4+u),(1/4+u),(1/4-u) $\bar{u}$, *u*, $\bar{u}$;$\bar{u}$, $\bar{u}$, *u*; (1/4+u),(1/4-u),(1/4+u);(1/4-u),(1/4+u),(1/4+u)

Table 3
Inversion parameters δ, Oxygen positional parameters, Residual functions *R* and Cation Distribution.

Composition (*x*)	**Distribution parameter (δ)**	**Oxygen positional parameter (*u*)**	**Residual function (*R*)**	**Cation distribution**					
				Tetrahedral site (A-site)			**Octahedral site (B-site)**		
				Co^{2+}	**Cu^{2+}**	**Fe^{3+}**	**Co^{2+}**	**Cu^{2+}**	**Fe^{3+}**
0.10	0.10	0.379	0.06	0.01	0.09	0.90	0.09	0.81	1.10
0.30	0.00	0.377	0.07	0.00	0.00	1.00	0.30	0.70	1.00
0.50	0.00	0.377	0.06	0.00	0.00	1.00	0.50	0.50	1.00
0.70	0.00	0.377	0.05	0.00	0.00	1.00	0.70	0.30	1.00
0.90	0.00	0.377	0.08	0.00	0.00	1.00	0.90	0.10	1.00

Table 4
Cation-anion, Anion-anion, and Cation-cation distances at A- and B-sites of $Co_xCu_{1-x}Fe_2O_4$.

X	***d_{TL}*(Å)**	***d_{OL}*(Å)**	***d_{TE}*(Å)**	***d_{OE}*(Å)**	***d_{OEU}*(Å)**	***d_A*(Å)**	***d_B*(Å)**
0.10	1.8634	2.0522	3.0430	2.8543	2.9494	3.6113	2.9486
0.30	1.8367	2.0708	2.9993	2.9050	2.9526	3.6156	2.9522
0.50	1.8394	2.0738	3.0036	2.9091	2.9568	3.6208	2.9564
0.70	1.8396	2.0740	3.0039	2.9095	2.9572	3.6213	2.9568
0.90	1.8415	2.0762	3.0072	2.9126	2.9603	3.6252	2.9599

Table 5
Magnetic moments of $Co_xCu_{1-x}Fe_2O_4$.

Composition	Magnetic moment of tetrahedral ions (μ_B)			Magnetic moment of octahedral ions (μ_B)			Magnetic moment per molecule (μ_B)
(X)	Co^{2+}	Cu^{2+}	Fe^{3+}	Co^{2+}	Cu^{2+}	Fe^{3+}	$Co_xCu_{1-x}Fe_2O_4$
0.1	0.03	0.09	4.5	0.27	0.81	5.5	1.96
0.3	0.00	0.00	5	0.9	0.7	5	1.60
0.5	0.00	0.00	5	1.5	0.5	5	2.00
0.7	0.00	0.00	5	2.1	0.3	5	2.40
0.9	0.00	0.00	5	2.7	0.1	5	2.80

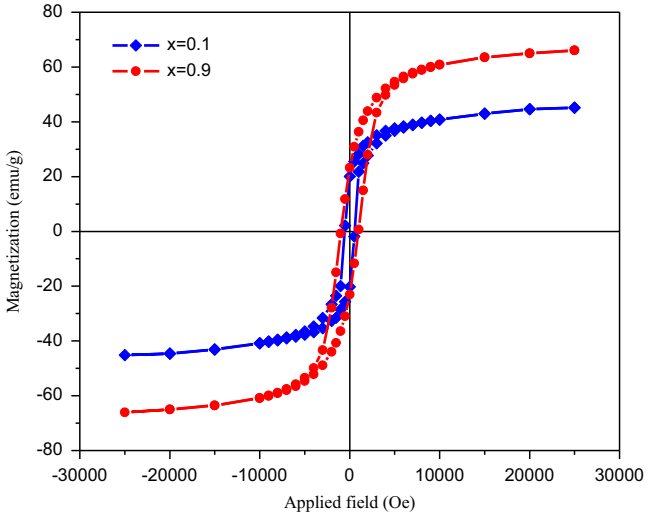

Fig. 6. *M–H* curves of $Cu_{1-x}Co_xFe_2O_4$ (for x=0.1and 0.9) ferrite nanoparticles samples at room temperature.

Table 6
The saturation magnetization (Ms), coercivity (Hc) and magnetic moment values of $Co_xCu_{1-x}Fe_2O_4$ (x=0.1 and 0.9) nanoparticles.

Composition	Saturation magnetization (Ms) emu/g	Coercivity (Hc) Oe	Magnetic moment (μ_B)
$Co_{0.1}Cu_{0.9}Fe_2O_4$	45.2	545	1.93
$Co_{0.9}Cu_{0.1}Fe_2O_4$	66.1	960	2.78

obtained hysteresis loops of the samples are shown in Fig. 6 and the calculated values of the experimental magnetic moments (μ_B) and the saturation magnetization are listed in Table 6. The values of Ms and Hc for $Cu_{1-x}Co_xFe_2O_4$ (x=0.1 and 0.9) increased with increasing Co concentration. The increase in saturation magnetization is due to the enhancement of the super-exchange interaction between the A and B-sites. As the cobalt concentration increases, the magnetization of the B-site increases and the net magnetization increase. The increase in Hc values with cobalt content may be due to the domain structure and anisotropy of the crystal. The experimental magnetic moment (μ_B) is determined from the saturation magnetization data using the following relation [24]: $\mu B = Mw \times Ms/5585$ where, M_W is the molecular weight of the sample and M_S is the saturation magnetization in emu/g.

4. Conclusion

In this work Co–Cu ferrite nanoparticles have been synthesized by the sol–gel technique, which is a much easier and advantageous way to synthesize nanoparticles. X-ray diffraction (XRD) analysis confirmed the fcc cubic phase development in the samples. The results indicated slight expansion in unit cell and decrease in density. Estimation of the distribution of cations carried out on the basis of X-ray diffraction (XRD), reveals that being inverse spinels both Cu and Co occupy the octahedral sites in spinel lattice. The proposed cation distribution is confirmed by the magnetic measurements and the theoretically suggested magnetic moment values are in good agreement with experimentally calculated ones.

References

[1] J.C. Waerenoborgh, M.O. Figucerido, J.M.P. Cabrol, L.C.J. Pereiro, Temperature and composition dependence of the cation distribution in synthetic $ZnFe_yAl_{2-y}O_4$ ($0 \le y \le 1$) spinels, Journal of Solid State Chemistry 111 (1994) 300–309.
[2] W. Bayoumi, Structural and electrical properties of zinc-substituted cobalt ferrite, Journal of Materials Science 42 (2007) 8254–8261.
[3] A. Goldman, Modern Ferrite Technology, second ed., Springer, Pittsburgh, 2006.
[4] P.K. Baltzer, P.J. Wojtowicz, M. Robbins, E. Lopatin, Exchange interactions in ferromagnetic chromium chalcogenide spinels, Physical Review 151 (1966) 367–377.
[5] A. Hussain, T. Abbas, S.B. Naizi, Preparation of $Ni_{1-x}Mn_xFe_2O_4$ ferrites by sol–gel method and study of their cation distribution, Ceramics International 07 (2012) 049〉.
[6] H. Furuhashi, M. Inagaki, S. Naka, Determination of cation distribution in spinels by X ray diffraction method, Journal of Inorganic and Nuclear Chemistry 35 (1973) 3009–3014.
[7] J.M. Rubio Gonzalez, C.O. Arean, X-Ray diffraction determination of the cation distribution and oxygen positional parameter in polycrystalline spinels, Journal of the Chemical Society, Dalton Transactions (1985) 2155–2159.
[8] E. Stoll, P. Fischer, W. Halg, G. Maier, Redetermination of the cation distribution of spinel. ($MgAl_2O_4$) by means of neutron diffraction, Journal de Physique Paris 25 (1964) 447–448.
[9] C.C. Wu, T.O. Mason, Thermopower composition dependence in ferrospinels, Journal of the American Ceramic Society 64 (1981) 520–522.
[10] U. Schmocker, H.R. Boesch, F. Waldner, A direct determination of cation: disorder in $MgAl_20_4$ spinel by ESR, Physics Letters A 40 (1972) 237–238.
[11] Q. Wei, J. Li, Y. Chen, Y. Han, X-ray study of cation distribution in $NiMn_{1-x}Fe_{2-x}$ O_4 ferrites, Materials Characterization 47 (2001) 247–252.
[12] D.R. Mane, U.N. Devatwal, K.M. Jadhav, Structural and magnetic properties of aluminium and chromium co-substituted cobalt ferrite, Materials Letters 44 (2000) 91–95.
[13] C. Nlebedim, N. Ranvah, P.I. Williams, Y. Melikhov, F. Anayi, J.E. Synder, A.J. Moses, D.C. Jiles, Influence of vacuum sintering on microstructure and magnetic properties of magnetostrictive cobalt ferrite, Journal of Magnetism and Magnetic Materials 321 (2009) 2528–2532.
[14] Ph. Tailhades, C. Villette, A. Rousset, G.U. Kulkarni, K.R. Kannan, Cation migration and coercivity in mixed copper–cobalt spinel ferrite powders, Journal of Solid State Chemistry 141 (1998) 56–63.
[15] A. Pradeep, G. Chandrasekaran, FTIR study of Ni, Cu and Zn substituted nano-particles of $MgFe_2O_4$, Materials Letters 60 (2006) 371–374.
[16] A. Pradeep, P. Priyadharsini, G. Chandrasekaran, Production of single phase nano size $NiFe_2O_4$ particles using sol–gel auto combustion route by optimizing the preparation conditions, Materials Chemistry and Physics 112 (2008) 572–576.
[17] T. Mathew, B.S. Rao, C.S. Gopinath, Tertiary butylation of phenol on $Cu_{1-x}Co_xFe_2O_4$: catalysis and structure-activity correlation, Journal of Catalysis 222 (2004) 107–116.
[18] Y. Khan, E. Kneller, Structure and magnetic moment of zinc-substituted γ iron oxide, Journal of Magnetism and Magnetic Materials 7 (1978) 9–11.

[19] J.A. Gomes, M.H. Sousa, G.J. da Silva, F.A. Tourinho, J. Mestnik-Filhoc, R. Itri, G.M. Azevedo, J. Depeyrot, Cation distribution in copper ferrite nanoparticles of ferrofluids, Journal of Magnetism and Magnetic Materials 300 (2006) 213–216.
[20] T. Meron, Y. Rosenberg, Y. Lereah, Synthesis and assembly of high-quality cobalt ferrite nanocrystals prepared by a modified sol–gel technique, Journal of Magnetism and Magnetic Materials 292 (2005) 11–16.
[21] M.I. Mendelson, Average grain size in polycrystalline ceramics, Journal of the American Ceramic Society 52 (1969) 443–446.
[22] K.E. Sickafus, J.M. Wills, N.W. Grimes, Structure of spinel, Journal of the American Ceramic Society 82 (1999) 3279–3292.
[23] I.S. Ahmed Farag, M.A. Ahmed, S.M. Hammad, A.M. Moustafa, Study of cation distribution in $Cu_{0.7}(Zn_{0.3-x}Mg_x)Fe_{1.7}Al_{0.3}O_4$ by X-ray diffraction using rietveld method, Egyptian Journal of Solids 24 (2001) 215–225.
[24] M.A. Gabal, Y.M. Al Angari, S.S. Al-Juaid, A study on Cu substituted Ni–Cu–Zn ferrites synthesized using egg-white, Journal of Alloys and Compounds 492 (1-2) (2010) 411–415.